Layer-by-Layer Assembly of Zeolite Crystals on Glass with Polyelectrolytes as Ionic Linkers

Goo Soo Lee, Yun-Jo Lee, and Kyung Byung Yoon*

Contribution from the Center for Microcrystal Assembly and Department of Chemistry, Sogang University, Seoul 121-742, Korea

Received February 26, 2001

Abstract: ZSM-5 crystals and glass plates tethered with trimethylpropylammonium iodide and sodium butyrate, respectively, (denoted as $\mathbf{Z}^+$, $\mathbf{Z}^-$, $\mathbf{G}^+$, and $\mathbf{G}^-$, respectively) were prepared. Treatment of $\mathbf{G}^-$ with $\mathbf{Z}^+$ suspended in ethanol results in monolayer assembly of $\mathbf{Z}^+$ on $\mathbf{G}^-$ ($\mathbf{G}^-/\mathbf{Z}^+$) with high surface coverage. The zeolite crystals have a strong tendency to closely pack and align with the *b*-axis normal to the glass plate, despite large positive ζ potentials. Subsequent treatment of $\mathbf{G}^-/\mathbf{Z}^+$ with $\mathbf{Z}^-$ leads to second-layer assembly of $\mathbf{Z}^-$ on $\mathbf{G}^-/\mathbf{Z}^+$ ($\mathbf{G}^-/\mathbf{Z}^+/\mathbf{Z}^-$), but with rather poor coverage. Sequential treatment of $\mathbf{G}^+$ with poly(sodium 4-styrenesulfonate) (Na^+PSS^-), poly(diallyldimethylammonium chloride) ($PDDA^+Cl^-$), and Na^+PSS^- followed by $\mathbf{Z}^+$ yields glass plates assembled with monolayers of $\mathbf{Z}^+$ with very high surface coverage through the composite polyelectrolyte linkers ($\mathbf{G}^+/PSS^-/PDDA^+/PSS^-/\mathbf{Z}^+$). The zeolite crystals also have a strong tendency to closely pack and align with the *b*-axis perpendicular to the substrate plane. The binding strength between the zeolite crystals and glass plates is much higher in $\mathbf{G}^+/PSS^-/PDDA^+/PSS^-/\mathbf{Z}^+$ than in $\mathbf{G}^-/\mathbf{Z}^+$. Repetition of the sequential $PSS^-/PDDA^+/PSS^-/\mathbf{Z}^+$ layering for five cycles yields glass plates assembled with pentalayers of ZSM-5 crystals [$\mathbf{G}^+/(PSS^-/PDDA^+/PSS^-/\mathbf{Z}^+)_5$]. The observed degrees of coverage and alignment of zeolite crystals in each layer were very high up to the third layers despite the nonuniformity of the sizes and shapes of the zeolite crystals used in this study. This report thus demonstrates the feasibility of layer-by-layer assembly of micrometer-sized zeolite crystals on glass through electrostatic interaction between surface-bound, full-fledged ionic centers, especially by use of polyelectrolyes as the linkers.

Introduction

Self-assembly of building blocks in the form of highly ordered arrays or thin films on various substrates is an effective way to organize building blocks into versatile functional entities, and this has been the focus of interest during the last several decades.[1,2] As modern chemistry is evolving away from the manipulation of sets of individual molecules toward the description and manipulation of systems of molecules,[3] the sizes of building blocks subjected to be assembled on substrates are currently experiencing an increase from subnanometer[4,5] to micrometer scales.[6−13] It is therefore highly necessary to develop novel methods to organize building blocks on the micrometer scales[6−13] or beyond[14−20] in the form of highly ordered multilayer arrays on substrates. Such methods will also be of great help in the development of nanotechnology,[21−25] which is of worldwide prime attention, since they will also provide insights into the assembly of nanobuilding blocks into three-dimensional functional entities. In fact, the ability to self-assemble building blocks in various length scales into functional entities is one of the marvelous features of biological systems.[26,27] Therefore, the development of such methods will also be of great help to provide insights into the biological phenomena.

We have been interested in the monolayer assembly of micrometer-sized zeolite crystals on substrates through well-

(1) Petty, M. C. *Langmuir-Blodgett Films: An Introduction*; Cambridge University Press: Cambrigde, UK, 1996.
(2) (a) Ulman, A., Fitzpatrick, L. E. Eds., *Characterization of Organic Thin Films*; Butterworth-Heinemann: Boston, MA, 1995. (b) Ulman, A. *An Introduction to Ultrathin Organic Films*; Academic Press: Boston, 1991. (c) Ulman, A. *Chem. Rev.* **1996**, *96*, 1533.
(3) Whitesides, G. M.; Ismagilov, R. F. *Science* **1999**, *284*, 89.
(4) Nuzzo, R. G.; Allara, D. L. *J. Am. Chem. Soc.* **1983**, *105*, 4481.
(5) Sagiv, J. *J. Am. Chem. Soc.* **1980**, *102*, 92.
(6) Kulak, A.; Lee, Y. J.; Park, Y. S.; Yoon, K. B. *Angew. Chem., Int. Ed.* **2000**, *39*, 950.
(7) Choi, S. Y.; Lee, Y.-J.; Park, Y. S.; Ha, K.; Yoon, K. B. *J. Am. Chem. Soc.* **2000**, *122*, 5201.
(8) Ha, K.; Lee, Y.-J.; Lee, H. J.; Yoon, K. B. *Adv. Mater.* **2000**, *12*, 1114.
(9) Lee, G. S.; Lee, Y.-J.; Ha, K.; Yoon, K. B. *Tetrahedron* **2000**, *56*, 6965.
(10) Ha, K.; Lee, Y.-J.; Jung, D.-Y.; Lee, J. H.; Yoon, K. B. *Adv. Mater.* **2000**, *12*, 1610.
(11) Kulak, A.; Park, Y. S.; Lee, Y.-J.; Chun, Y. S.; Ha, K.; Yoon, K. B. *J. Am. Chem. Soc.* **2000**, *122*, 9308.
(12) Ha, K.; Lee, Y.-J.; Chun, Y. S.; Park, Y. S.; Lee, G. S.; Yoon, K. B. *Adv. Mater.* **2001**, *13*, 594.
(13) Ha, K.; Chun, Y. S.; Kulak, A.; Park, Y. S.; Lee, Y.-J.; Yoon, K. B. *Stud. Surf. Sci. Catal.* **2001**. In press.
(14) Bowden, N.; Terfort, A.; Carbeck, J.; Whitesides, G. M. *Science* **1997**, *276*, 233.
(15) Huck, W. T. S.; Tien, J.; Whitesides, G. M. *J. Am. Chem. Soc.* **1998**, *120*, 8267.
(16) Choi, I. S.; Bowden, N.; Whitesides, G. M. *J. Am. Chem. Soc.* **1999**, *121*, 1754.
(17) Bowden, N.; Choi, I. S.; Grzybowski, B. A.; Whitesides, G. M. *J. Am. Chem. Soc.* **1999**, *121*, 5373.
(18) Weck, M.; Choi, I. S.; Jeon, N. L.; Whitesides, G. M. *J. Am. Chem. Soc.* **2000**, *122*, 3546.
(19) Gracias, D. H.; Tien, J.; Breen, T. L.; Hsu, C.; Whitesides, G. M. *Science* **2000**, *289*, 1170.
(20) Choi, I. S.; Weck, M.; Jeon, N. L.; Whitesides, G. M. *J. Am. Chem. Soc.* **2000**, *122*, 11997.
(21) Mirkin, C. A. *Inorg. Chem.* **2000**, *39*, 2258.
(22) Alivisatos, A. P. *Science* **2000**, *289*, 736.
(23) Yeadon, M.; Ghaly, M.; Yang, J. C.; Averback, R. S.; Gibson, J. M. *Appl. Phys. Lett.* **1998**, *73*, 3208.
(24) Peyser, L. A.; Vinson, A. E.; Bartko, A. P.; Dickson, R. M. *Science* **2001**, *291*, 103.
(25) (a) Penn, R. L.; Banfield, J. F. *Science* **1998**, *281*, 969. (b) Banfield, J. F.; Welch, S. A.; Zhang, H.; Ebert, T. T.; Penn, R. L. *Science* **2000**, *289*, 751.

10.1021/ja010517q CCC: $20.00
Published on Web 09/13/2001

defined covalent bonds.[6−13] The zeolite crystals in the assembled monolayers show a tendency to align in one direction and closely pack between themselves. The aligned and closely packed monolayers are useful even for their own sakes since they are expected to be widely applied in industry as well-defined zeolite thin films.[28−37] The monolayers of zeolite crystals also bear a great potential to be employed as organizing media for various semiconductor quantum dots in a highly ordered and oriented way.[22−25,38,39] Despite the great applicability of the zeolite monolayers, one should eventually come up with the methods to assemble micrometer-sized zeolite crystals into multilayers, hopefully with uniform alignment, for more versatile application of the assembled multilayer zeolite thin films. This is also important from the point of view of biomineralization processes[40] and ceramic materials science.[41,42] However, despite our continual efforts to assemble multilayers,[13] the binding strengths between the substrates and zeolite crystals based on the covalent linkers that have been developed thus far are not strong enough to allow multilayer assembly of zeolite crystals on substrates. We now demonstrate layer-by-layer (multilayer) assembly of micrometer-sized zeolite crystals on glass plates by ionic interaction between the surface-bound full-fledged ionic centers, by employing multiple, alternately layered oppositely charged polyelectrolytes as the linker, with excellent degrees of coverage and close packing in each layer up to the third layers.

Experimental Section

Materials. Zeolite-A with the average size of ~0.4 μm was synthesized according to the literature procedures.[43] ZSM-5 with the average crystal size of 2.0 × 1.5 × 0.8 μm^3 (large ZSM-5) was synthesized from a gel with the molar ratio of TEOS:TPAOH:$NaAlO_2$:H_2O = 10:1:0.05:600, where TEOS and TPAOH represent tetraethyl orthosilicate and tetrapropylammonium hydroxide, respectively, and the composition of $NaAlO_2$ was Na_2O = 31−35% and Al_2O_3 = 34−39%. TEOS (26.6 g) was first introduced into TPAOH solution (12.7 g of 1 M TPAOH diluted in 117 g of water) followed by addition of sodium aluminate solution (1%, 8.7 g). The final clear gel was stirred for 12 h at room temperature and transferred to an autoclave, and the synthesis was carried out with stirring with the aid of a magnetic stirrer at 135 °C for 40 h. The ZSM-5 with the average crystal size of 1.0 × 0.7 × 0.4 μm^3 (medium ZSM-5) was synthesized from a gel with the molar ratio of TEOS:TPAOH:$NaAlO_2$:H_2O = 6:1:0.05:460. TEOS (17.6 g) was introduced into TPAOH solution (14 g of 1 M TPAOH diluted in 97 g of water) followed by addition of sodium aluminate solution (1%, 5.8 g). The gel was stirred for 12 h at room temperature. The final clear gel was transferred to an autoclave, and the synthesis was carried out with stirring at 180 °C for 12 h. The ZSM-5 with the average crystal size of 0.3 × 0.2 × 0.1 μm^3 (small ZSM-5) was synthesized from a gel with the molar ratio of TEOS:TPAOH:$NaAlO_2$:H_2O = 7:1:0.06:280. TEOS (25 g) was introduced into TPAOH solution (20 g of 1 M TPAOH diluted in 76 g of water) followed by addition of sodium aluminate solution (1%, 9.8 g). The gel was aged for 8 days at room temperature. The final clear gel was transferred to an autoclave, and the synthesis was carried out with stirring at 180 °C for 12 h. The obtained ZSM-5 crystals were thoroughly washed with copious amounts of water. The template ions such as tetramethylammonium (TMA^+) and tetrapropylammonium (TPA^+) employed to synthesize zeolite-A and ZSM-5, respectively, were removed by calcining at 550 °C for 12 h under flowing oxygen prior to treatment with silylating agents.

(3-Aminopropyl)triethoxysilane (AP-TES) from Aldrich was distilled and kept in a Schlenk storage flask under argon. (3-Cyanopropyl)-trichlorosilane (CNP-TCS) and [3-(2,3-epoxypropoxy)propyl]trimethoxysilane (EPP-TMS) from Merck were used as received. For simplicity, 3-aminopropyl, 3-cyanopropyl, and 3-(2,3-epoxypropoxy)propyl are denoted as AP, CNP, and EPP, respectively. Poly(sodium 4-styrenesulfonate) (Na^+PSS^-, M_w 70000), poly(diallyldimethylammonium chloride) ($PDDA^+Cl^-$, 20 wt % in water, ~M_w 100000−200000), and polyethylenimine (PEI, M_w 25000) were purchased from Aldrich and used as received. Cover glasses (18 × 18 mm^2) were purchased from Marienfeld and treated in a piranha solution (H_2SO_4:30% H_2O_2 = 3:1) at 95−100 °C for 1 h to remove organic residues on the surface. The acid-treated glasses were washed with distilled deionized water and dried at 120 °C for 30 min prior to treatment with CNP-TCS or AP-TES. Optical grade fused silica plates were purchased from CVI Laser Co., and the surfaces of them were similarly cleaned with piranha solution prior to treatment with CNP-TCS. All the organic solvents were purified according to the well-known literature procedures prior to use.

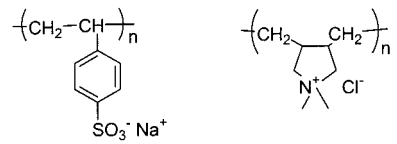

Na^+PSS^- $PDDA^+Cl^-$

Preparation of AP-Tethering Zeolite-A and ZSM-5 Crystals (Scheme 1, Step I). Dry toluene (50 mL) was introduced into a Schlenk flask containing zeolite-A or ZSM-5 (100 mg) under argon, and the heterogeneous mixture was sonicated for 10 min in an ultrasonic cleaner to evenly disperse zeolite particles in toluene. AP-TES (0.5 mL) was injected into the toluene slurry with the aid of a hypodermic syringe under the counter flow of argon, and the mixture was refluxed for 1 h under argon. After cooling to room temperature, the AP-tethering

(26) Whitesides, G. M. *Sci. Am.* **1995**, *273*, 146.
(27) Ozin, G. A. *Chem. Commun.* **2000**, 419.
(28) (a) Feng, S.; Bein, T. *Nature* **1994**, *368*, 834. (b) Feng, S.; Bein, T. *Science* **1994**, *265*, 1839. (c) Yan, Y.; Bein, T. *J. Am. Chem. Soc*. **1995**, *117*, 9990. (d) Yan, Y.; Bein, T. *J. Phys. Chem.* **1992**, *96*, 9387. (e) Bein, T. *Chem. Mater*. **1996**, *8*, 1636.
(29) (a) Boudreau, L. C.; Tsapatsis, M. *Chem. Mater*. **1997**, *9*, 1705. (b) Gouzinis, A.; Tsapatsis, M. *Chem. Mater*. **1998**, *10*, 2497. (c) Boudreau, L. C.; Kuck, J. A.; Tsapatsis, M. *J. Membr. Sci*. **1999**, *152*, 41. (d) Xomeritakis, G.; Tsapatsis, M. *Chem. Mater*. **1999**, *11*, 875.
(30) (a) Lassinantti, M.; Hedlund, J.; Sterte, J. *Microporous Mesoporous Mater*. **2000**, 38, 25. (b) Engström, V.; Mihailova, B.; Hedlund, J.; Holmgren, A.; Sterte, J. *Microporous Mesoporous Mater*. **2000**, 38, 51. (c) Hedlund, J.; Minotova, S.; Sterte, J.; *Microporous Mesoporous Mater*. **1999**, *28*, 185. (d) Hedlund, J.; Noack, M.; Kölsch, P.; Creaser, D.; Caro, J.; Sterte, J. *J. Membr. Sci.* **1999**, 159, 263. (e) Mihailova, B.; Engström, V.; Hedlund, J.; Holmgren, A.; Sterte, J. *Microporous Mesoporous Mater.* **1999**, *32*, 297.
(31) (a) Clet, G.; Jansen, J. C.; van Bekkum, H. *Chem. Mater*. **1999**, *11*, 1696. (b) van der Puil, N.; Dautzenberg, F. M.; van Bekkum, H.; Jansen, J. C. *Microporous Mesoporous Mater*. **1999**, *27*, 95. (c) Jansen, J. C.; Koegler, J. H.; van Bekkum, H.; Calis, H. P. A.; van den Bleek, C. M.; Kapteijn, F.; Moulijn, J. A.; Geus, E. R.; van den Puil, N. *Microporous Mesoporous Mater*. **1998**, *21*, 213. (d) Koegler, J. H.; van Bekkum, H.; Jansen, J. C.; *Zeolites* **1997**, *19*, 262.
(32) (a) Muñoz, T., Jr.; Balkus, K. J., Jr. *Chem. Mater*. **1998**, *10*, 4114. (b) Muñoz, T., Jr.; Balkus, K. J., Jr. *J. Am. Chem. Soc*. **1999**, *121*, 139.
(33) Li, Z.; Lai, C.; Mallouk, T. E. *Inorg. Chem*. **1989**, *28*, 178.
(34) (a) Caro, J.; Finger, G.; Kornatowski, J. *Adv. Mater*. **1992**, *4*, 273. (b) Caro, J.; Noack, M.; Richter-Mendau, J.; Marlow, F.; Petersohn, D.; Griepentrog, M.; Kornatowski, J. *J. Phys. Chem*. **1993**, *97*, 13685. (c) Noack, M.; Kölsch, P.; Venzke, D.; Toussaint, P.; Caro, J. *Microporous Mesoporous Mater*. **1994**, *3*, 201. (d) Kölsch, P.; Venzke, D.; Noack, M.; Lieske, E.; Toussaint, P.; Caro, J. *Stud. Surf. Sci. Catal*. **1994**, *84*, 1075.
(35) Plog, C.; Maunz, W.; Kurzwei, P.; Obermeir, E.; Scheilbe, C. *Sens. Actuators, B* **1995**, *24*−*25*, 403.
(36) Chau, J. L. H.; Tellez, C.; Yeung, K. L.; Ho, K. *J. Membr. Sci*. **2000**, *164*, 257.
(37) Ban, T.; Ohwaki, T.; Ohya, Y.; Takahashi, Y. *Angew. Chem., Int. Ed.* **1999**, 38, 3324.
(38) (a) Ozin, G. A. *Adv. Mater*. **1992**, *4*, 612. (b) Ozin, G. A.; Kuperman, A.; Stein, A. *Angew. Chem., Int. Ed. Engl*. **1989**, *28*, 359.
(39) Stucky, G. D.; MacDougall, J. E. *Science* **1990**, *247*, 669.
(40) (a) Mann, S., Webb, J., Williams, R. J. P., Eds. *Biomineralization*; VCH: NewYork, 1989. (b) Lowenstam, H. A.; Weiner, S. *On Biomineralization*; Oxford University Press: Oxford, 1989. (c) Vincent, J. F. V. *Structural Biomaterials*; Macmillan: London, 1982. (d) Wainwright, S. A.; Biggs, W. D.; Currey, J. D.; Gosline, J. M. *Mechanical Design in Organisms*; Edward Arnold: London, 1976.
(41) Weiner, S.; Addadi, L. *J. Mater. Chem*. **1997**, *7*, 689.
(42) Stupp, S. I.; Braun, P. V. *Science* **1997**, *277*, 1242.
(43) Zhu, G.; Qiu, S.; Yu, J.; Sakamoto, Y.; Xiao, F.; Xu, R.; Terasaki, O. *Chem. Mater*. **1998**, *10*, 1483.

Scheme 1

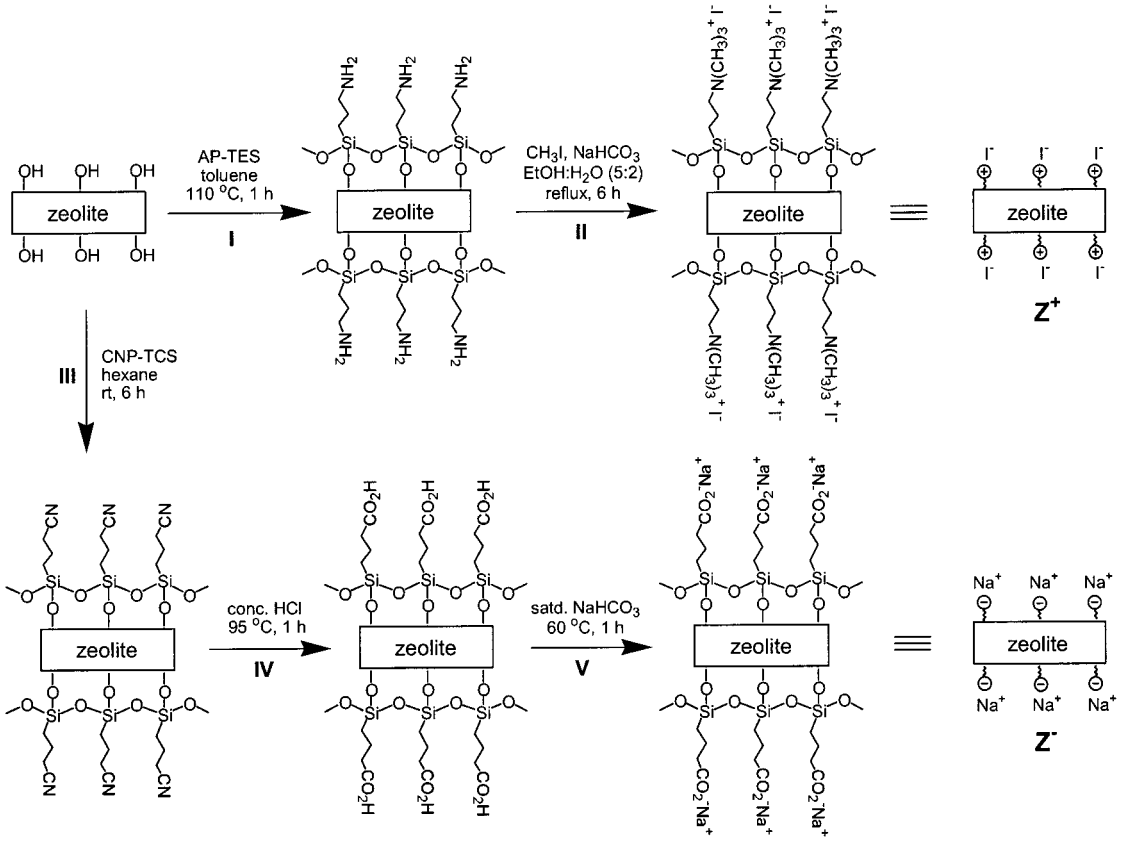

zeolite powders were collected by rapid filtration in the atmosphere over a filter paper. The filter papers were wetted with toluene prior to filtration. The collected powders were successively washed with fresh toluene (100 mL) and ethanol (100 mL). The collected powders were dried for 30 min in an oven at 120 °C.

Permethylation of Zeolite-Bound AP Groups to Quaternary Ammonium Salts (Scheme 1, Step II). Ethanol (40 mL) and an aqueous sodium bicarbonate solution (1 mL of saturated $NaHCO_3$ diluted in 15 mL of distilled deionized water) were consecutively introduced into a round-bottomed flask containing zeolite-A or ZSM-5 tethered with AP (100 mg). Sonication (10 min) was applied to disperse the zeolite crystals within the solution. Iodomethane (1 mL) was added into the mixture, and it was refluxed for 6 h. The mixture was then cooled to room temperature, and the zeolite powders tethering trimethylpropylammoinum iodide ($TMPA^+I^-$) were collected by rapid filtration over a filter paper in the atmosphere. The collected $TMPA^+I^-$-tethering zeolite powders were successively washed with fresh ethanol (100 mL) and water (100 mL) and subsequently dried for 30 min in an oven at 120 °C. The $TMPA^+I^-$-tethering ZSM-5 is symbolized as indicated in Scheme 1 and designated as $\mathbf{Z}^+$.

Preparation of CNP-Tethering ZSM-5 Crystals (Scheme 1, Step III). Rigorously dried hexane (50 mL) was introduced into a Schlenk flask containing ZSM-5 (100 mg) under argon, and the heterogeneous mixture was sonicated for 10 min to evenly disperse zeolite particles into the solvent. CNP-TCS (0.5 mL) was injected into the hexane mixture with the aid of a hypodermic syringe under a counter flow of argon, and the mixture was stirred at room temperature for 6 h under an argon atmosphere. The CNP-tethering zeolite powders were collected by rapid filtration in the atmosphere over a filter paper. The filter papers were wetted with hexane prior to filtration. The collected powders were successively washed with fresh hexane (100 mL) and ethanol (100 mL) and subsequently dried for 30 min in an oven at 120 °C.

Hydrolysis of CNP Groups Bound to ZSM-5 to Butyric Acid (Scheme 1, Step IV). Hydrochloric acid (concentrated, 50 mL) was introduced into a flask containing the CNP-tethering ZSM-5 crystals. The mixture was warmed to 95 °C and kept at the temperature for 1 h. After cooling to room temperature, the ZSM-5 crystals tethered with butyric acid (BuA) groups were collected by filtration over two overlapped filter papers (Whatman No. 1 at the top and No. 5 at the bottom) and washed with copious amounts of water. The washed BuA-tethering ZSM-5 crystals were dried for 30 min in an oven at 120 °C. (This procedure is not applicable to zeolite-A since the basic zeolite is not stable in such a highly acidic medium.)

Transformation of BuA Groups Bound to ZSM-5 into Sodium Butyrate (Scheme 1, Step V). The BuA-tethering ZSM-5 crystals were introduced into a solution of saturated sodium carbonate (50 mL), and the mixture was warmed to 60 °C. The mixture was kept for 1 h at the same temperature. After cooling to room temperature, the ZSM-5 crystals tethered with sodium butyrate (Na^+Bu^-) were collected by filtration and washed with copious amounts of water. The washed Na^+Bu^--tethering ZSM-5 crystals were dried for 30 min in an oven at 120 °C. The Na^+Bu^--tethering ZSM-5 is symbolized as indicated in Scheme 1 and designated as $\mathbf{Z}^-$.

Preparation of $TMPA^+I^-$-Tethering Glass Plates (G^+). The glass plates tethered with $TMPA^+I^-$ groups were prepared by employing the successive procedures applied for preparation of $\mathbf{Z}^+$ (Scheme 1) by employing 10 pieces of glass plate instead of zeolite crystals. A $TMPA^+I^-$-tethering glass plate is symbolized as the following and designated as $\mathbf{G}^+$.

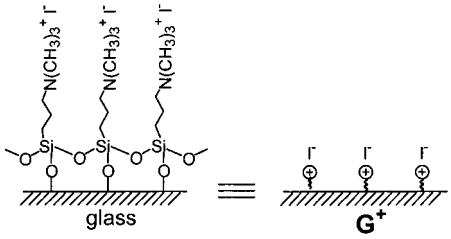

Preparation of Na^+Bu^--tethering Glass Plates (G^-). The glass plates tethered with Na^+Bu^- groups were prepared by employing the procedures for preparation of $\mathbf{Z}^-$ by using 10 pieces of glass plate instead of ZSM-5 and by reducing the amount of CNP-TCS from 0.5

to 0.1 mL. A glass plate tethering Na^+Bu^- is symbolized as the following and designated as $\mathbf{G}^-$.

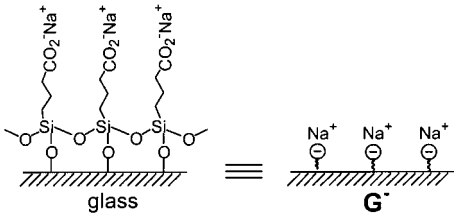

Assembly of Z^+ on G^- by Direct Electrostatic Interaction (G^-/Z^+). Ethanol (50 mL) was introduced into a flask containing $\mathbf{Z}^+$ (either zeolite-A or ZSM-5, 30 mg). The flask was sonicated for 10 min to evenly disperse the zeolite crystals into the solvent. A Teflon support containing 10 pieces of $\mathbf{G}^-$ was immersed into the ethanol solution, and the mixture was shaken for 1 h at 60 °C. After cooling to room temperature, the glass plates coated with zeolite crystals were removed from the flask, washed with ethanol, and dried in an oven at 120 °C for 30 min. The glass plates were sonicated in toluene for 30 s to remove physisorbed zeolite crystals over the electrostatically assembled monolayers of zeolite crystals. The glass plate assembled with a monolayer of $\mathbf{Z}^+$ is designated as $\mathbf{G}^-/\mathbf{Z}^+$ and symbolized as the following. For convenience, slash "/" is used in this paper to denote interface between the contacting layers.

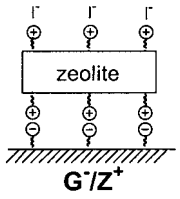

Preparation of $G^-/Z^+/Z^-$. Ethanol (50 mL) was introduced into a flask containing $\mathbf{Z}^-$ (30 mg). The flask was then sonicated for 10 min to disperse the zeolite crystals into the solution. A Teflon support containing 10 pieces of $\mathbf{G}^-/\mathbf{Z}^+$ was immersed into the ethanol suspension of $\mathbf{Z}^-$, and the solution was shaken for 1 h at 60 °C. The glass plates coated with double layers of ZSM-5 crystals ($\mathbf{G}^-/\mathbf{Z}^+/\mathbf{Z}^-$) were removed from the flask and washed with ethanol and dried in an oven at 120 °C for 30 min. The glass plates were sonicated in toluene for 30 s to remove physisorbed zeolite crystals.

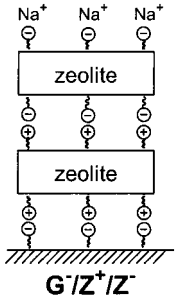

Formation of Monolayers of Z^+ on G^+ with PSS^- as the Linker ($G^+/PSS^-/Z^+$) (Scheme 2, Paths I and II). Na^+PSS^- (0.21 g, 1 mmol) was dissolved in an aqueous solution of sodium chloride (0.1 M, 50 mL). The mole of the polymer is based on the moles of the repeating units. Ten pieces of $\mathbf{G}^+$ were immersed into the aqueous saline solution of PSS^-. The use of saline solution for dissolution of PSS^- was intended to induce even coating of the electrolyte on the glass plates according to the results of Hammond et al.[44] After 20 min of dipping, the glass plates layered with PSS^- ($\mathbf{G}^+/\mathbf{PSS}^-$) were removed from the flask, rinsed with copious amounts of water, and dried by exposing them to a gentle stream of high purity nitrogen. Ten pieces of $\mathbf{G}^+/\mathbf{PSS}^-$ were immersed into an ethanol suspension of $\mathbf{Z}^+$ (30 mg, in 50 mL of ethanol), and the mixture was stirred for 1 h at 60 °C. After cooling to room temperature, the glass plates coated with $\mathbf{Z}^+$ ($\mathbf{G}^+/\mathbf{PSS}^-/\mathbf{Z}^+$) were removed, washed with ethanol, and dried for 30 min in an oven at 120 °C. The glass plates were sonicated in toluene for 30 s to remove physisorbed zeolite crystals.

Preparation of $G^+/PSS^-/PDDA^+/Z^-$ (Scheme 2, Paths III and IV). $PDDA^+Cl^-$ (0.8 mL of 20% solution, 1 mmol) was dissolved in an aqueous solution of sodium chloride (0.1 M, 50 mL). Into the saline solution of $PDDA^+Cl^-$, 10 pieces of $\mathbf{G}^+/\mathbf{PSS}^-$ were immersed. After 20 min of dipping, the glass plates layered with $PSS^-/PDDA^+Cl^-$ ($\mathbf{G}^+/\mathbf{PSS}^-/\mathbf{PDDA}^+$) were removed from the flask, rinsed with copious amounts of water, and dried by exposing them to a gentle stream of high-purity nitrogen. Ten pieces of $\mathbf{G}^+/\mathbf{PSS}^-/\mathbf{PDDA}^+$ were immersed into an ethanol suspension of $\mathbf{Z}^-$ (30 mg in 50 mL of ethanol) and the mixture was shaken for 1 h at 60 °C. After cooling to room temperature, the glass plates coated with $\mathbf{Z}^-$ ($\mathbf{G}^+/\mathbf{PSS}^-/\mathbf{PDDA}^+/\mathbf{Z}^-$) were removed, washed with ethanol, dried, and sonicated for 30 s in toluene to remove physisorbed zeolite crystals.

Preparation of $G^+/PSS^-/PDDA^+/PSS^-/Z^+$ (Scheme 2, Paths V and VI). Ten pieces of $\mathbf{G}^+/\mathbf{PSS}^-/\mathbf{PDDA}^+$ were immersed for 20 min into the saline solution of Na^+PSS^- prepared above. After removal from the solution, the resulting $\mathbf{G}^+/\mathbf{PSS}^-/\mathbf{PDDA}^+/\mathbf{PSS}^-$ plates were washed with copious amounts of water and dried. The glass plates ($\mathbf{G}^+/\mathbf{PSS}^-/\mathbf{PDDA}^+/\mathbf{PSS}^-$) were immersed into an ethanol suspension of $\mathbf{Z}^+$ (30 mg in 50 mL of ethanol), and the mixture was shaken for 1 h at 60 °C. After cooling to room temperature, the glass plates coated with $\mathbf{Z}^+$ were removed, washed, dried, and sonicated for 30 s in toluene to remove physisorbed zeolite crystals.

Assembly of Multilayers of Z^+ on G^+ with $PSS^-/PDDA^+/PSS^-$ as the Repeating Linker. Assembly of bilayers $[\mathbf{G}^+/(\mathbf{PSS}^-/\mathbf{PDDA}^+/\mathbf{PSS}^-/\mathbf{Z}^+)_2]$, trilayers $[\mathbf{G}^+/(\mathbf{PSS}^-/\mathbf{PDDA}^+/\mathbf{PSS}^-/\mathbf{Z}^+)_3]$, and pentalayers $[\mathbf{G}^+/(\mathbf{PSS}^-/\mathbf{PDDA}^+/\mathbf{PSS}^-/\mathbf{Z}^+)_5]$ of $\mathbf{Z}^+$ on $\mathbf{G}^+$ through $\mathbf{PSS}^-/\mathbf{PDDA}^+/\mathbf{PSS}^-$ composite polyelectrolyte multilayers was carried out by repeating the desired number of cycles of the monolayer assembly as illustrated in Scheme 3 for trilayer assembly.

Comparison of the Linkage-Dependent Binding Strength between Zeolite Crystals and Glass Plates. The linkage-dependent binding strengths between zeolite crystals and glass plates were compared by monitoring the progressive loss of zeolite crystals from the glass plates as a result of increasing the length of sonication in toluene. Sonication of the samples was carried out using an ultrasonic cleaning bath. Each sample was sonicated for 30 s to remove physisorbed zeolite particles prior to weight loss profile. After each desired period of sonication (1 min for the first 10 min, then 5 min for the remaining 50 min), the weight of each glass plate was measured on a microbalance (Mettler MT5). The details about the procedure can be found from our previous report.[11] For comparison, we also prepared ZSM-5 monolayers assembled on the glass plates by two different types of covalent linkages; the direct linkages between the zeolite-bound AP and glass-bound EPP groups and the multiple linkages between EPP groups bound to both zeolite crystals and glass plates through interlinking PEI. They are denoted as **G−EPP−AP−Z** and **G−EPP−PEI−EPP−Z**, respectively. The procedures to assemble monolayers of zeolite crystals on glass plates through amine−EPP linkages are described in our previous reports.[6,11]

Instrumentation. The scanning electron microscope (SEM) images of zeolites and the zeolite-coated glass plates were obtained from a FE-SEM (Hitachi S-4300) at an acceleration voltage of 10−20 kV. A platinum/palladium alloy (in the ratio of 8 to 2) was deposited with a thickness of about 15 nm on top of the samples. The X-ray diffraction patterns for the identification of the zeolite crystals were obtained from a Rigaku diffractometer (D/MAX-1C) with the monochromatic beam of Cu Kα. The diffuse reflectance UV−vis spectra of solid samples were obtained using an integrating sphere (Varian Cary-5). FT-IR spectra were recorded on a JASCO FT/IR-620. The water contact angles of the modified glass plates were measured on a contact angle goniometer (Rame-Hart model 100). The values were taken from six different regions within a sample and 15 s after water (2 μL) was dropped. The reported values thus stand for the averages. Sonication of the samples was carried out using an ultrasound cleaning bath operated at 28 kHz. ζ potentials of zeolite samples ($\mathbf{Z}^+$ and $\mathbf{Z}^-$, and

(44) Clark, S. L.; Montague, M. F.; Hammond, P. T. *Macromolecules* **1997**, *30*, 7237.

Scheme 2

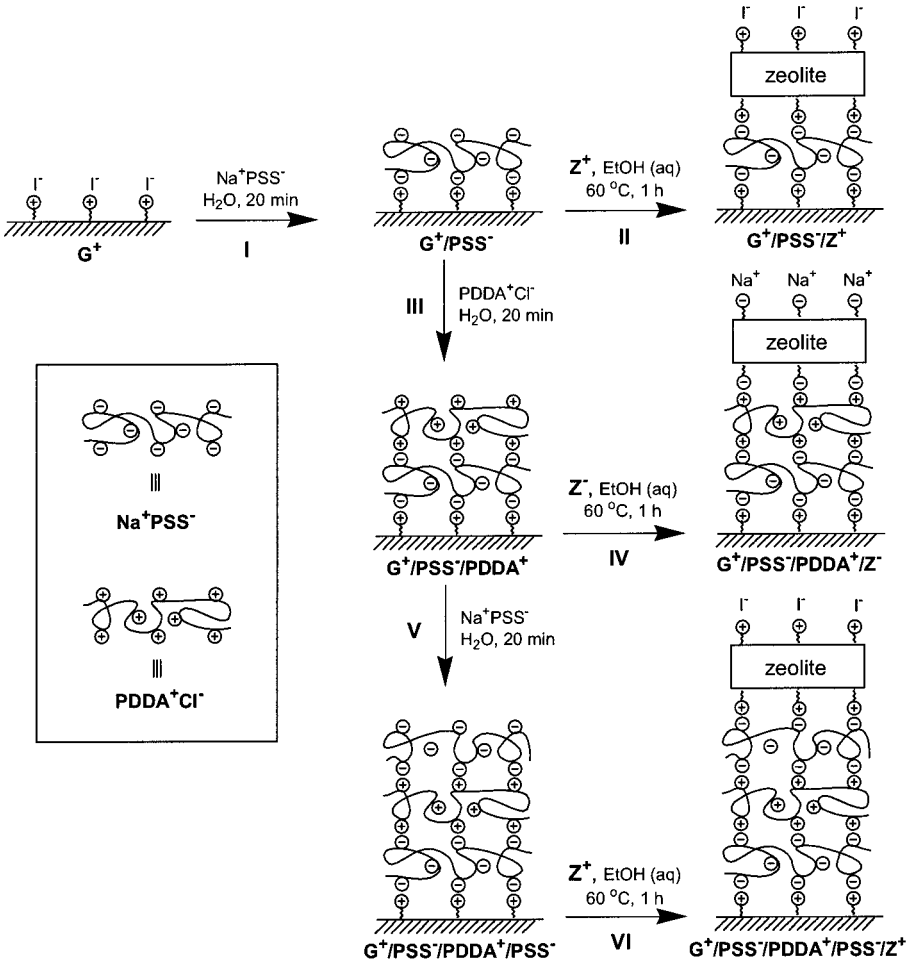

ZSM-5) were measured on a Malvern Zetasizer 3000. The concentration of zeolite in ethanol was 0.17 g L^{-1}, and 5 mL of each sample was injected into the flow cell.

Results and Discussion

Preparation of Z^+. The AP-tethering zeolite crystals were prepared according to step 1 in Scheme 1. The presence of AP groups on the zeolite surfaces was confirmed by the positive ninhydrin test as described in our previous report.[7] The subsequent permethylation of the zeolite-bound AP groups with methyl iodide readily yielded quaternary ammonium centers. The appearance of the characteristic absorption band of iodide at 220 nm in the diffuse reflectance UV−vis spectrum of the zeolite crystals confirmed the presence of charge-balancing iodide[45,46] in $TMPA^+I^-$ groups (see Supporting Information). The disappearance of the absorption band upon exchanging the iodide with chloride or acetate through aqueous ion exchange and ready restoration of the band upon reexchange of the chloride or acetate with iodide further confirms the presence of $TMPA^+I^-$ groups.

Preparation of G^-. As a means to confirm the ready attachment of CNP groups onto glass we employed glass beads (~μm) instead of glass plates and the diffuse reflectance FT-IR spectra of the CNP-TCS-treated glass beads were taken (see Supporting Information). The FT-IR spectra of the CNP-TCS-treated glass beads show the C−H stretching bands as 2941 and 2889 cm^{-1} and the C≡N stretching band at 2245 cm^{-1}. The nitrile-stretching band disappears after treatment of the CNP-tethering glass beads with HCl, while the C−H stretching bands remain intact at 2939 and 2885 cm^{-1}. The concomitant appearance of the broad O−H stretching bands centered at 3645 and 3367 cm^{-1} and C═O stretching band at 1693 cm^{-1} confirms the conversion of CNP to BuA groups. The stretching band at 1537 cm^{-1} may arise due to the C−O single-bond stretching band. Upon neutralization of the BuA groups with sodium bicarbonate, the carbonyl stretching band shifted to the lower-energy region (1589 cm^{-1}) consistent with the general trend of the C═O stretching bands upon transformation of the terminal carboxylic acid to alkali metal salt of carboxylate. The presence of strong C−H stretching bands at 2952 and 2881 cm^{-1} further confirms the presence of a propyl linkage between the glass and sodium carboxylate. The above results thus confirm the ready transformation of CNP groups to Na^+Bu^- via BuA groups (Scheme 1). Consistent with the progressive increase in the hydrophilicity of the terminal group, the water contact angle decreased from 57° to 34° and to 25° upon changing the tethered groups from CNP to BuA and to Na^+Bu^-, respectively.

Assembly of Monolayers of Z^+ on G^-. Upon mixing, crystals of Z^+ readily assemble in the form of monolayers on G^-. Such an assembly does not occur when CNP groups tethered to glass plates are not transformed into Na^+Bu^- groups or AP groups bound to zeolite crystals are not transformed into $TMPA^+I^-$. This strongly suggests that the monolayer assembly occurs by ion exchange of the Na^+ ions in the ion pairs of Na^+Bu^- tethered to glass plates with $TMPA^+$ ions in $TMPA^+I^-$ attached to zeolite crystals. The positive silver ion test of the

(45) Blandamer, M. J.; Fox, M. F. *Chem. Rev.* **1970**, *70*, 59.
(46) Sheu, W. S.; Rossky, P. J. *J. Am. Chem. Soc.* **1993**, *115*, 7729.

Scheme 3

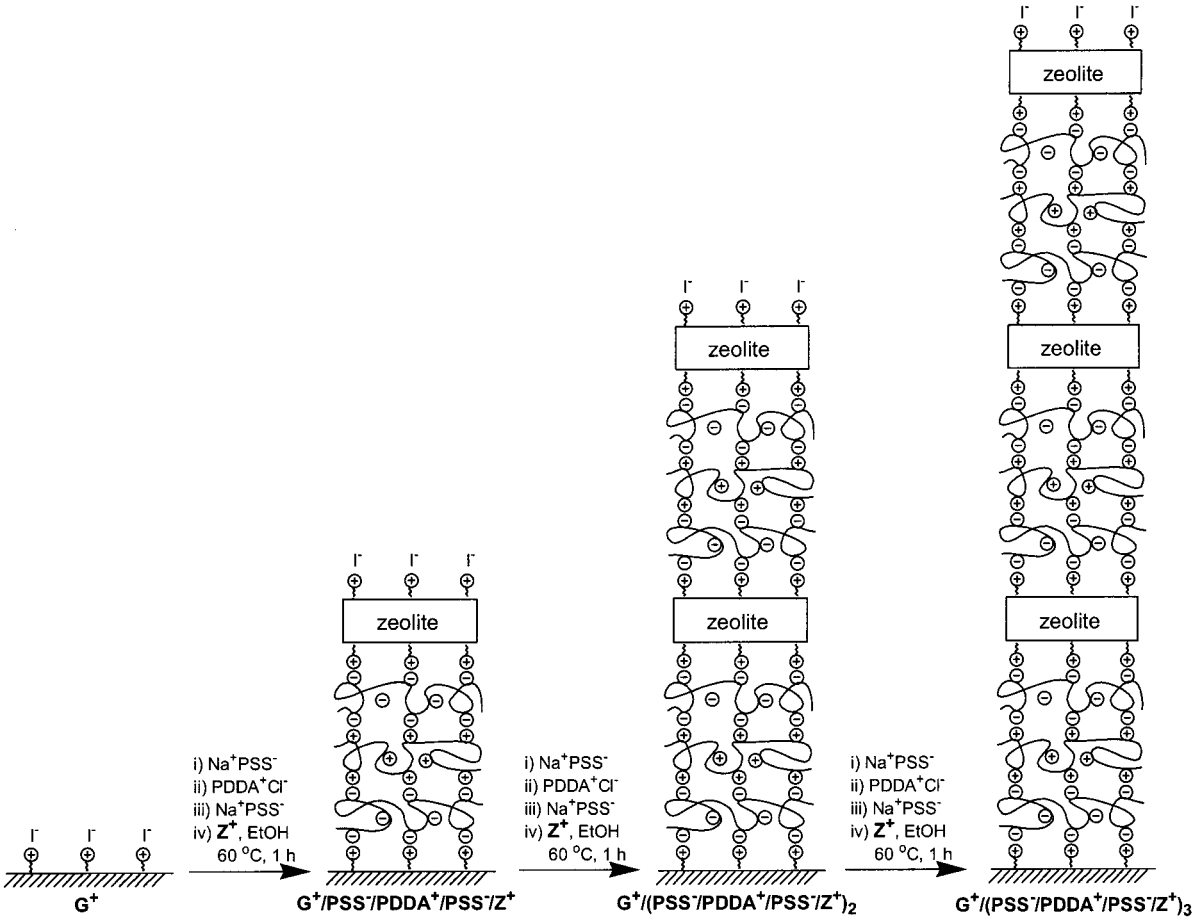

ethanol solution from a large-scale experiment confirmed liberation of iodide into the solution. The typical scanning electron microscopy (SEM) images of $\mathbf{G}^-/\mathbf{Z}^+$ are shown in Figure 1 (panels A and B), before (A) and after (B) brief (30 s) sonication. Panel A shows that only a small amount of $\mathbf{Z}^+$ crystals (<10%) are physically adsorbed on top of the monolayers of $\mathbf{Z}^+$ that are bound to $\mathbf{G}^-$ through electrostatic interaction. The X-ray diffraction patterns of $\mathbf{G}^-/\mathbf{Z}^+$ shown in each inset of panels A and B, respectively, show diffraction patterns of only (0 k 0) reflections for $k = 2$, 4, 6, 8, and 10 at $2\theta = 8.9$, 17.8, 26.8, 36.0, and 45.5°. This indicates that even the physically adhered zeolite particles are aligned parallel to the surface of $\mathbf{G}^-$, consistent with the SEM image (Figure 1A). Thorough inspection of the glass plates shows that the glass plates are entirely covered with the monolayers of $\mathbf{Z}^+$ with similar degrees of close packing. The images also show the strong propensity of $\mathbf{Z}^+$ for packing closely. The cubic zeolite-A crystals tethered with $TMPA^+I^-$ also readily form the corresponding monolayers on $\mathbf{G}^-$.

The profile of the sonication-induced zeolite loss from the glass plates (Figure 2A) revealed that the binding strength between ZSM-5 crystals and glass plates is much stronger with the $Bu^-/TMPA^+$ ionic linkages than with the covalent EPP-AP linkages. Such a dramatic increase in the binding strength indicates that the number of linkages is higher for ionic linkages than it is for covalent linkages, under the assumption that the nature of the linkage (whether it is ionic or N−C covalent linkage) does not greatly affect the binding strengths. This result may reflect that ionic linkages are much more favorable than covalent linkages. This is conceivable in the sense that ionic bonding is nondirectional or omnidirectional and can also tolerate slight variation in the distance between the positive and negative centers, while covalent linkages require stringent angles and distances for the approaching functional groups for successful formation of linkages. However, from the fact that the binding strength between $\mathbf{G}^-$ and $\mathbf{Z}^+$ is still weaker than that of EPP−PEI−EPP multiple covalent linkage, the number of $Bu^-/TMPA^+$ ionic linkages between the two uneven surfaces of glass and zeolite is still less than that of the multiple PEI-mediated covalent linkages.[11]

Assembly of ZSM-5 Bilayers on Glass through direct $TMPA^+/Bu^-$ Ionic Linkages ($\mathbf{G}^-/\mathbf{Z}^+/\mathbf{Z}^-$). We also independently prepared $\mathbf{Z}^-$ according to the procedure shown in Scheme 1 and attempted layering of $\mathbf{Z}^-$ on top of the monolayers of $\mathbf{Z}^+$ via direct $TMPA^+/Bu^-$ ionic linkages. As a result, we were able to layer monolayers of $\mathbf{Z}^-$ on top of the monolayers of $\mathbf{Z}^+$ as typically shown in Figure 1C. However, the degree of the second-layer coverage was not uniform throughout the glass plates, and there are many domains with poor second-layer coverage as typically shown in Figure 1D. The poor second-layer coverage is likely to arise primarily from the increased degree of roughness of the underlying (first) layer due to the uneven thickness of the ZSM-5 crystals and the presence of some ZSM-5 crystals with protruding twinned crystals on top of the flat zeolite faces ($a-c$ planes). As a result, we suspect that the number of $TMPA^+/Bu^-$ ionic linkages is not large enough to tightly hold the second-layer zeolite crystals on top of the first layer. In this regard, as a means to increase the number of ionic linkages, we employed polyelectrolytes as the linkers as described in the next section.

Assembly of Monolayers of $\mathbf{Z}^+$ on $\mathbf{G}^+$ via Multilayers of Oppositely Charged Polyelectrolytes. We independently pre-

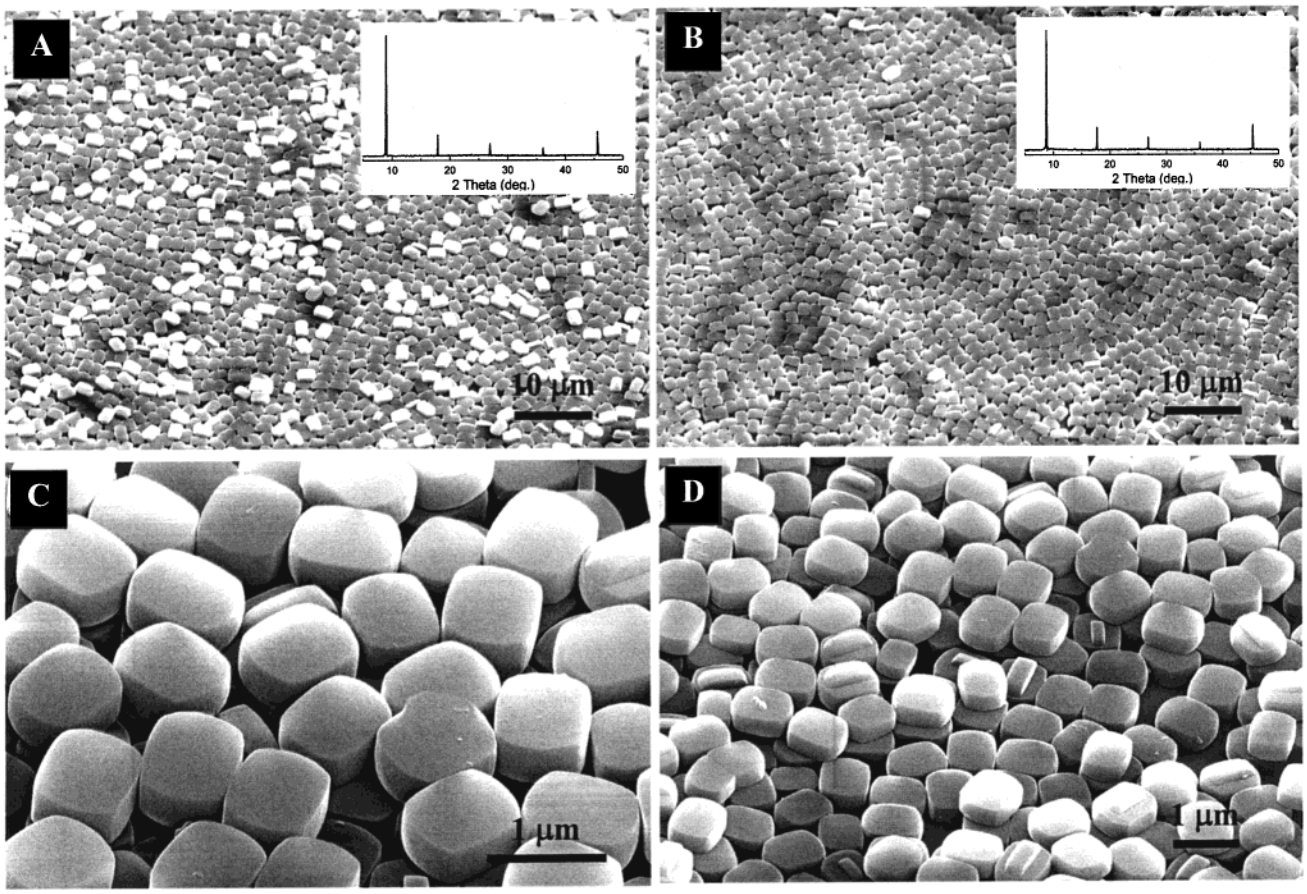

Figure 1. SEM images of $\mathbf{G}^-$ treated with $\mathbf{Z}^+$ before (A) and after (B) sonication (30 s). The insets show the corresponding X-ray diffraction pattern of the zeolite crystals. C and D represent the SEM images of $\mathbf{G}^-/\mathbf{Z}^+/\mathbf{Z}^-$ in the densely (C) and scarcely (D) packed area.

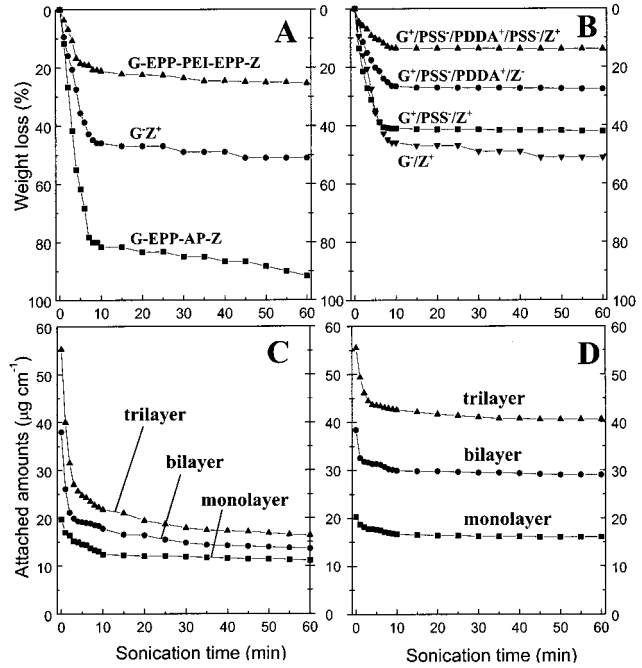

Figure 2. Comparison of sonication-induced weight (zeolite) loss profiles; the zeolite monolayers with three (A) and four (B) different types of linkage between zeolite crystals and glass plates, the glass plates with three different layers of zeolite crystals before (C) and after calcination at 550 °C for 12 h (D) (as indicated).

pared $\mathbf{G}^+$, and on top of it PSS^- was layered according to Path I in Scheme 2 to test PSS^- as the polyelectrolyte linker for the monolayer assembly of $\mathbf{Z}^+$ on $\mathbf{G}^+$. The ready attachment of $TMPA^+I^-$ groups on glass was indirectly confirmed by employing fused silica plates as the substrates instead of glass plates. Indeed, the UV−vis spectra of the fused silica plates treated with AP-TES and methyl iodide showed the iodide absorption band at 220 nm (see Supporting Information). When PSS^- was layered on the $TMPA^+I^-$-tethering fused silica plates ($\mathbf{S}^+$), the UV−vis spectra of the fused silica plates revealed the characteristic absorption band of PSS^- centered at 225 nm consistent with the presence of phenyl moieties in PSS^- (see Supporting Information). The subsequent treatment of the PSS^--layering fused silica plates ($\mathbf{S}^+/\mathbf{PSS}^-$) or glass plates ($\mathbf{G}^+/\mathbf{PSS}^-$) with $\mathbf{Z}^+$ readily yielded monolayers of $\mathbf{Z}^+$ on the substrates as revealed by the SEM images that look similar to the one shown in Figure 1B. Comparison of the sonication-induced zeolite-detachment profiles showed that the binding strength between the zeolite crystals and substrates increases upon employing PSS^- as the interfacial ionic linker as shown in Figure 2, although the increase is small.

Consecutively, we prepared $\mathbf{G}^+/\mathbf{PSS}^-/\mathbf{PDDA}^+$ and $\mathbf{G}^+/\mathbf{PSS}^-/\mathbf{PDDA}^+/\mathbf{PSS}^-$ and the corresponding fused silica analogues $\mathbf{S}^+/\mathbf{PSS}^-/\mathbf{PDDA}^+$ and $\mathbf{S}^+/\mathbf{PSS}^-/\mathbf{PDDA}^+/\mathbf{PSS}^-$ for UV−vis analysis according to Paths III and V, respectively, in Scheme 2 and proceeded with the assembly of the corresponding monolayers of either $\mathbf{Z}^-$ or $\mathbf{Z}^+$ on the corresponding oppositely charged glass plates according to Paths IV and VI, respectively. The 2-fold increase of the absorption of PSS^- from $\mathbf{S}^+/\mathbf{PSS}^-/\mathbf{PDDA}^+/\mathbf{PSS}^-$ with respect to that from $\mathbf{S}^+/\mathbf{PSS}^-$ confirms the ready stratification of the polyelectrolytes as we intended (see Supporting Information). The binding strength progressively increases with increasing the number of polyelectrolyte layers as shown in Figure 2B. Thus, the sonication-induced detached

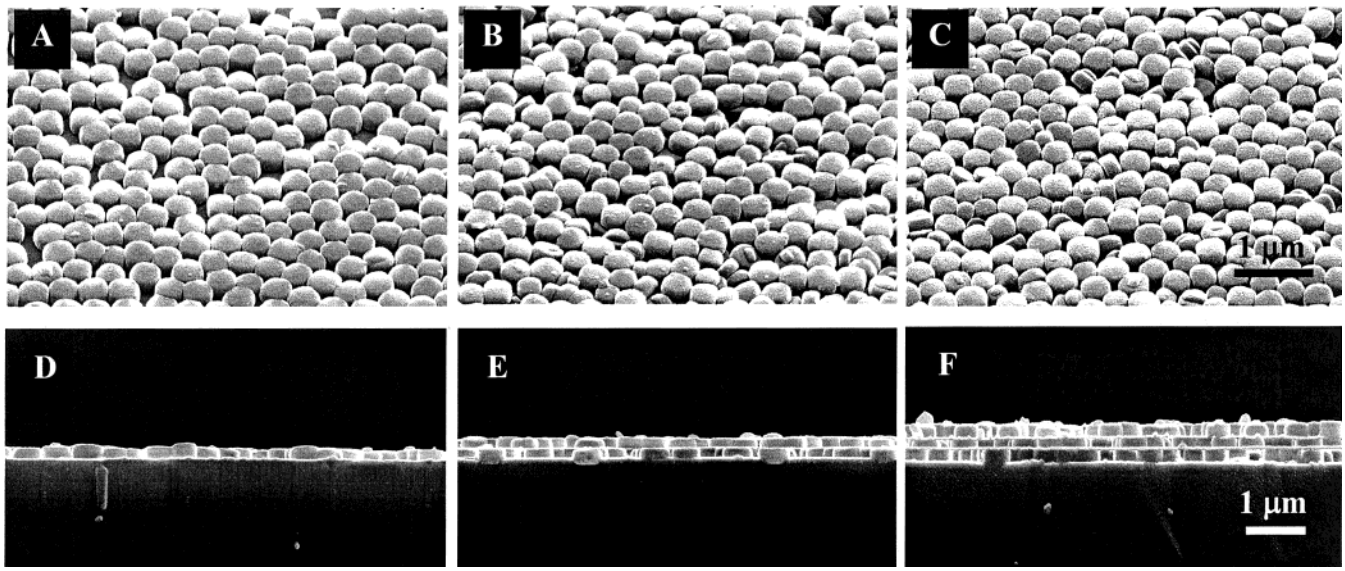

Figure 3. SEM images of the outermost layers of $\mathbf{G^+/(PSS^-/PDDA^+/PSS^-/Z^+)}$ (A), $\mathbf{G^+/(PSS^-/PDDA^+/PSS^-/Z^+)_2}$ (B), and $\mathbf{G^+/(PSS^-/PDDA^+/PSS^-/Z^+)_3}$ (C), and the corresponding cross sections (D, E, and F).

amount of ZSM-5 crystals reduced from 50 to 42, 28, and 14% with increasing the number of polyelectrolyte layers from none to 1, 2, and 3. This result coincides well with our previous results that introduction of polymeric linkers leads to the increase of the binding strength between the zeolite crystals and glass plates with microscopically uneven surfaces.[11,13] Interestingly, upon employing $PSS^-/PDDA^+/PSS^-$ composite layers as the interfacial linkers, the binding strength between the ZSM-5 crystals and glass plates exceeds that of ZSM-5 crystals linked to glass by the EPP−PEI−EPP linkages (compare panels A and B in Figure 2). Although we did not investigate, the increase in the number of polyelectrolyte layers may lead to a further increase in the binding strength.

Assembly of Trilayer of Z^+ on G^+ with $PSS^-/PDDA^+/PSS^-$ as Repeating Linker $[G^+/(PSS^-/PDDA^+/PSS^-/Z^+)_3]$. Knowing the fact that the use of $PSS^-/PDDA^+/PSS^-$ trilayer as the linker gives rise to a marked increase in the binding strength between $\mathbf{G}^+$ and $\mathbf{Z}^+$ we further attempted layer-by-layer assembly of ZSM-5 crystals on glass plates according to Scheme 3. For this experiment we used small ZSM-5 crystals. The perspective SEM images of the outermost layers of $\mathbf{G^+/(PSS^-/PDDA^+/PSS^-/Z^+)_}x$ for $x = 1$, 2, and 3 are shown in Figure 3, together with the corresponding images of the cross sections. This is the first case in which the assembly of multilayers of zeolite crystals beyond double layers was successful for us. This result is reproducible, and the SEM images of the trilayers of ZSM-5 crystals at lower magnifications (Figure 4, panels A and B) reveal that the entire glass plates are covered with the trilayers with similar degrees of coverage and lateral close packing. There are some defect sites as typically shown in Figure 4C, which also shows the trilayer assembly of $\mathbf{Z}^+$. Interestingly, all three zeolite layers remained intact even after they were shaken for 1 day in an aqueous 1 M solution of NaCl or $CaCl_2$. This indicates that the interaction between the oppositely charged organic ions is thermodynamically more favorable than that between the organic and inorganic ions.

As can be noticed from the SEM images shown in Figures 3 and 4C (right), the zeolite crystals align with their *b*-axis normal to the surface of glass plates, despite the fact that the degree of unevenness of the underlying layer increases significantly upon increasing the number of layers. Consistent with this, the X-ray diffraction pattern of the glass plates revealed only (0 *k* 0) reflections regardless of the number of layers (Figure 5). However, the diffraction intensity did not increase linearly with respect to the number of layers. For instance, the resulting intensities of the (0 2 0) diffraction were 1700, 3342, and 4872 cps for the monolayer, bilayer, and trilayer, respectively, indicating that the degree of coverage for each layer decreases with increasing numbers of layers. Consistent with this, the measured average weights of zeolite crystals for each layer are 19.7, 18.2, and 17.1 μg cm^{-1}, for the first, second, and third layer, respectively.

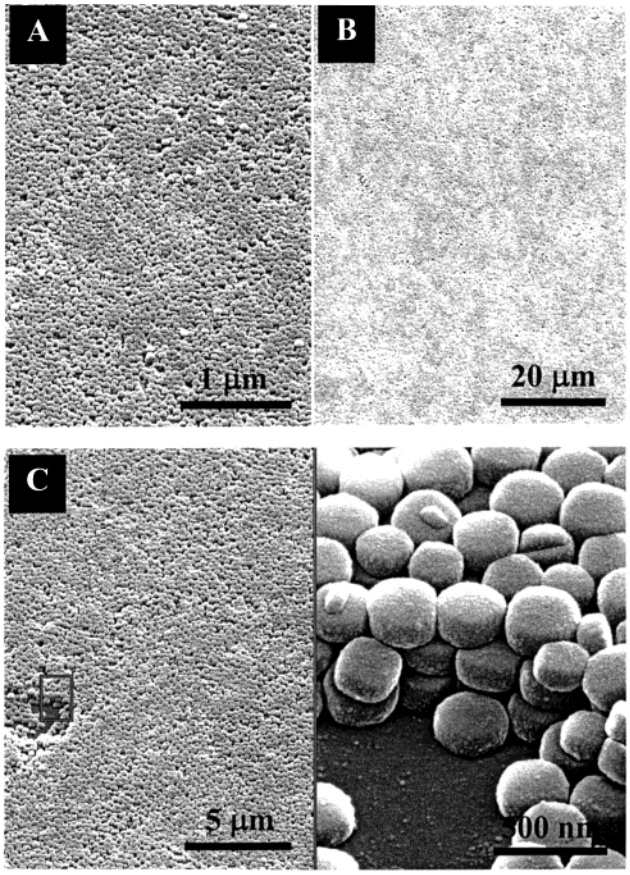

Figure 4. SEM images of $\mathbf{G^+/(PSS^-/PDDA^+/PSS^-/Z^+)_3}$ in two different low magnifications (A and B) and a defected site (C).

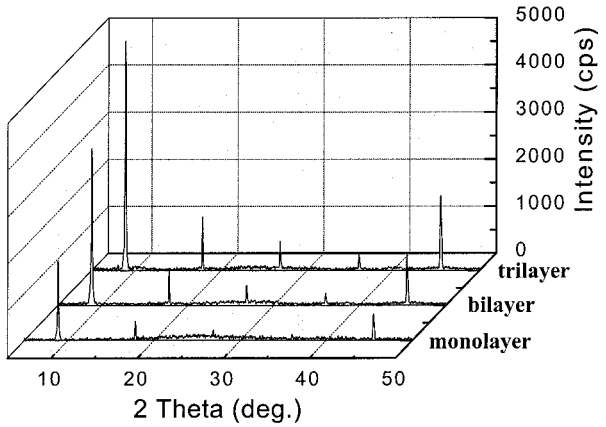

Figure 5. X-ray diffraction patterns of $\mathbf{G^+/(PSS^-/PDDA^+/PSS^-/Z^+)}$ (A), $\mathbf{G^+/(PSS^-/PDDA^+/PSS^-/Z^+)_2}$ (B), and $\mathbf{G^+/(PSS^-/PDDA^+/PSS^-/Z^+)_3}$ (C), as indicated.

On the basis of this, the degree of zeolite coverage decreases to 91 and 85% on going from the first to the second and the third layer, with respect to that of the first layer.

The sonication-induced zeolite-detachment profiles are shown in Figure 2C. The detached amounts during the first 5-min period of sonication were 5.1, 19.0, and 29.8 μg cm^{-1}, for the monolayer, bilayer, and trilayer of zeolite crystals, respectively. The total detached amounts from the glass plates assembled with monolayer, bilayer, and trilayer after 1-h sonication were 9.0, 24.7, and 39.0 μg cm^{-1}, respectively, which correspond to detachment of zeolite by 45, 60, and 65%, respectively, with respect to the corresponding initial amount. Thus, it is quite evident that the binding strength decreases as the number of layers increases. Interestingly, after calcination at 550 °C for 12 h, the binding strength increases markedly, as the corresponding detachment profiles show in Figure 2D. The calcined glass plates are expected to be useful for preparation of continuous zeolite films with controlled thickness through secondary growth.

Assembly of $[\mathbf{G^+/(PSS^-/PDDA^+/PSS^-/Z^+)_5}]$. Having been successful with the assembly of trilayers of $\mathbf{Z^+}$ on $\mathbf{G^+}$ by use of PSS$^-$/PDDA$^+$/PSS$^-$ composite polyelectrolytes as the linker, we repeated the cycle for five times, and the resulting glass plates were analyzed by SEM. It was revealed that pentalayers of $\mathbf{Z^+}$ indeed assemble on the glass plates but with larger areas of defected sites than trilayers. The typical SEM images of an outermost layer and a cross section of a pentalayer are shown in Figure 6 (panels A and B, respectively). This result thus confirms that the assembly of even $\mathbf{G^+/(PSS^-/PDDA^+/PSS^-/Z^+)_5}$ is also feasible. However, as can be seen in Figure 6A, randomly oriented ZSM-5 crystals are readily detectable among the crystals aligned with the *b*-axis normal to the plane of the substrate. Consistent with the SEM images, the measured X-ray diffraction patterns of the glass plates revealed the presence of diffraction patterns that correspond to (1 0 1), (0 1 1), (3 0 3), and (5 0 1), due to the presence of randomly oriented crystals, together with the (0 *k* 0) planes as shown in Figure 6C. The diffraction patterns of (*h* 0 0) planes with $h = 6$, 8, and 10 are likely to arise from the twined crystals protruding from the parent ZSM-5 crystals with the *a*-axis perpendicular to the $a-c$ plane of the parent crystals. The appearance of the (*h* 0 0) diffraction patterns from the pentalayers, which was not apparent from the trilayers, seems to be the result of higher intensities of the diffraction patterns as a result of higher number of layers of zeolite crystals. The absence of (2 0 0) and (4 0 0) planes in Figure 6C is due to the overlap of the planes with the corresponding (0 2 0) and (0 4 0) planes since the angle difference between (*h* 0 0) and (0 *k* 0) planes decreases as the diffraction angle decreases. The observed intensity of the (0 2 0) plane was 7940 cps, which still corresponds to 467% of that of the first layer. This result indicates that the coverage of pentalayers is still high, despite the presence of larger areas with defect sites. The appearance of larger defect sites from the pentalayers suggests that pentalayer is about the highest multilayer that can be assembled using the zeolite crystals we have employed in this study. However, we believe assembly of even higher layers can be achieved, provided that the zeolite crystals have clearer-cut facets and are monodisperse with respect to the sizes and morphologies.

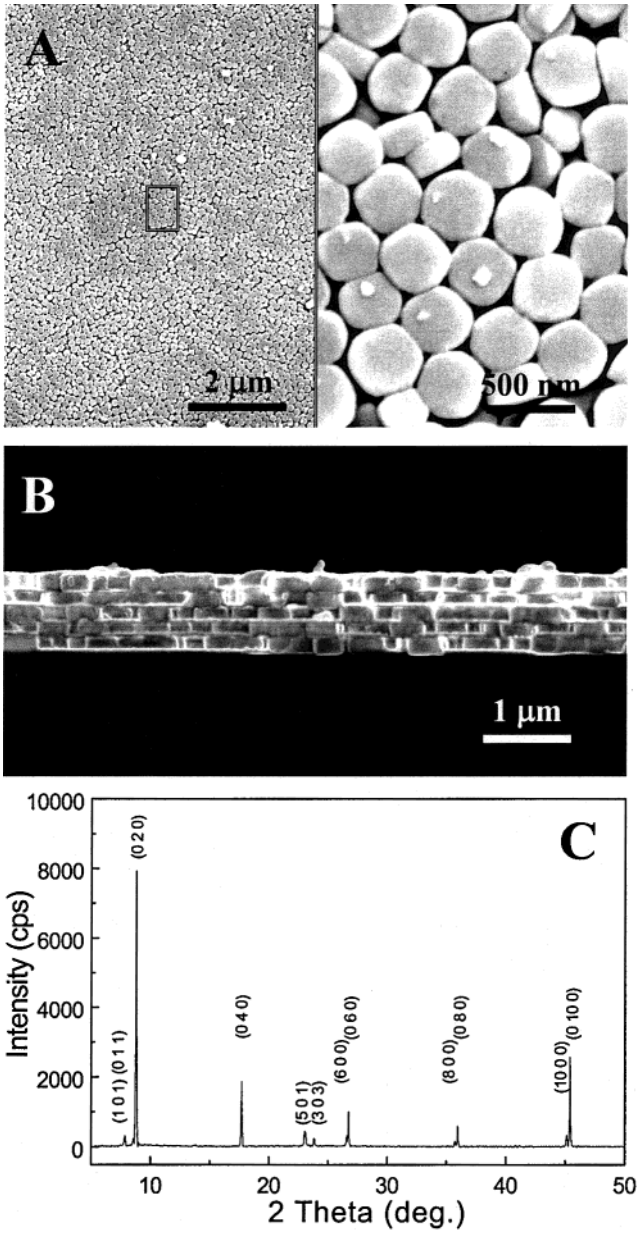

Figure 6. Typical SEM images of the outermost layer of $\mathbf{G^+/(PSS^-/PDDA^+/PSS^-/Z^+)_5}$ (A) and the corresponding cross section (B) and a typical X-ray diffraction pattern of glass plates assembled with pentalayers of $\mathbf{Z^+}$ (C).

Advantage of Employing Full-Fledged Charge Centers. Polyelectrolytes have been employed for the monolayer assembly of seed zeolite crystals on substrates for preparation of zeolite thin films through secondary growth.[28−30] For this purpose, polyamines or protonated polyamines have usually been

layered on the substrates. For instance, Tsapatsis et al.[29c] demonstrated attachment of bare (plain) zeolite-A crystals onto AP-tethering silicon wafers by use of PSS^- and polyallylamine-HCl adduct as the linkers. In their case, the zeolite crystals do not closely pack despite high coverage. Furthermore, low pH is necessary to maintain positive charges on the substrate-bound amine groups, while high pH is beneficial to maintain negative ζ potential on zeolite. Obviously, such conditions are mutually deleterious. Therefore, their observation of the decrease in the coverage with exposure time is likely to arise from self-neutralization. Their result contrasts with ours since longer exposure does not affect the degree of coverage in our case. It is also important to note that only poor and inhomogeneous coverage of zeolite results if quarternization of the surface-bound AP groups is omitted (see Supporting Information). Furthermore, even the poorly assembled zeolite crystals readily fell off upon brief sonication (<30 s). On the basis of the above contrasting results, we believe that the use of full-fledged charge centers such as $TMPA^+$ and Bu^- as well as polyelectrolytes with full-fledged charge centers such as $PDDA^+$ and PSS^- are crucial for inducing strong binding between zeolite crystals and glass substrates, which ultimately enables multilayer assembly of zeolite crystals on substrates. The measured ζ potentials of $\mathbf{Z}^+$ and $\mathbf{Z}^-$ are +50 and −49 mV, respectively, and the absolute values of them are larger than that of bare ZSM-5 crystals (−36 mV). We found that the use of ethanol which is less polar than water is also beneficial for high surface coverage, while maintaining the close packing of zeolite crystals.

Facile Surface Migration of Zeolite Crystals for Close Packing. The SEM images of the monolayers of zeolite crystals shown in Figure 1, A and B and Figure 3A clearly show that the zeolite crystals have strong tendency to closely pack next to each other despite high ζ potentials. Such a tendency prevailed even among the zeolite crystals being layered in the second and third layers, despite the degree of surface unevenness of the underlying layers increases dramatically. To gain insight into the procedure for such lateral close packing, we took out the glass plates at the intermediate stages of zeolite assembly and analyzed them with SEM. For this experiment, the monolayer assembly of $\mathbf{Z}^+$ on $\mathbf{G}^-$ was chosen. We found that the zeolite crystals randomly dot the glass plates at the very beginning of assembly (see Supporting Information). This indicates that the glass plates do not have preferred sites for the incoming zeolite crystals. Therefore, the zeolite crystals land on the substrate randomly, as one would expect. As time passes by, however, clusters of closely packed zeolite crystals begin to form on the surface. The clusters grow larger with time and as a result they start merging and eventually cover the entire glass surface with close packing.

Scrutiny of the glass plates reveals that there are many domains in which the crystals pack in the same three-dimensional orientation. In other words, so-called "oriented attachment"[21,22] operates during the assembly. The oriented attachment is more clearly visible in the case of zeolite-A crystals with cubic morphologies. The tendency of oriented attachment among nanometer-sized crystals has been well documented, and such a phenomenon has been described as one of the unique properties of nanoparticles during their assembly. This work clearly demonstrates that even the micrometer-sized crystals show a strong tendency to maintain maximum contact between the crystals.

As a means to be more objective and precise in elucidating the pattern of zeolite packing, we employed large ZSM-5 crystals to make the individual zeolite crystals visible through optical microscopes. Observation of the glass plates through optical microscopes is necessary to monitor the progress of zeolite assembly on the same spots, since optical microscopy does not require conductive coating of the samples with Pd/Pt or Au, which gives rise to permanent bonding of the particles onto the substrates.

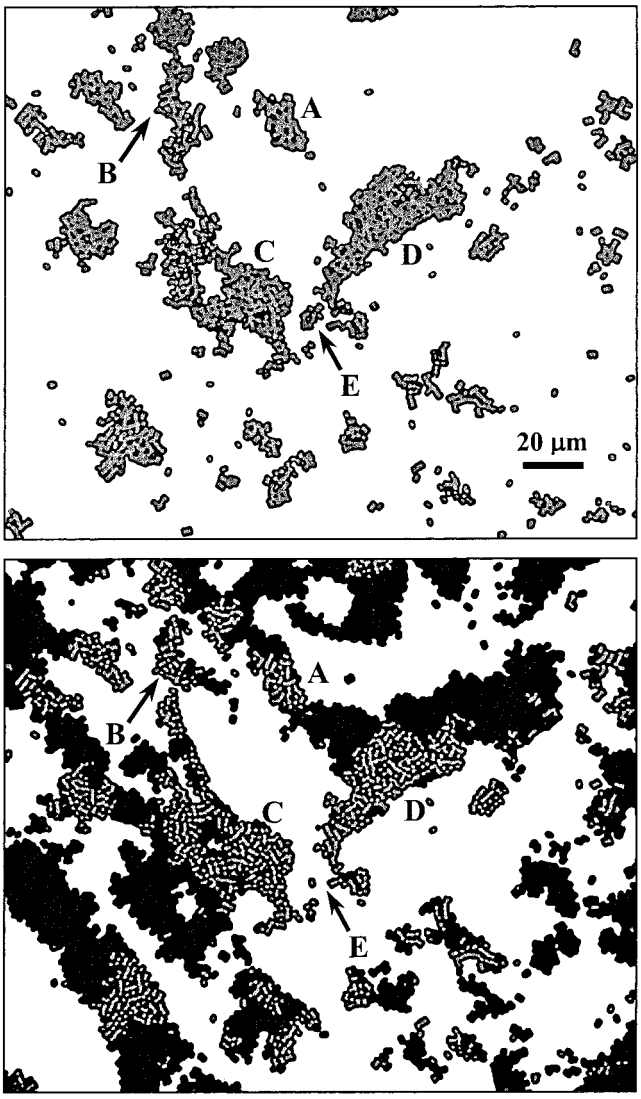

Figure 7. Optical microscope images of a fixed spot in a piece of $\mathbf{G}^-$ attached with ZSM-5 crystals ($\mathbf{Z}^+$) at two intermediate stages during monolayer assembly.

Figure 7A shows the scattered islands of closely packed zeolite crystals on a glass plate at an intermediate stage of monolayer assembly. This figure also shows that the number of isolated individual zeolite crystals is very low. Five islands with different sizes and shapes are labeled as indicated. Figure 7B shows that the newly introduced crystals do not grow isotropically around the preexisting islands but grow only in certain directions. The reason for such anisotropic growth remains to be elucidated. It is noticed that the island A becomes connected to the island above it and to island D by the newly attached closely packed zeolite crystals. The new crystals also attach along the edge of the internal void space of island C, and new void space is also created within the newly appearing closely packed zeolite crystals at the bottom of the island. Interestingly, some zeolite crystals that were parts of an island also become detached from the glass substrate, as noticed in island B that fragments into three pieces. Most of the zeolite

crystals forming the small island E also disappeared during the same period of time. There are also many newly appearing islands as noticed in Figure 7B. Scrutiny of the closely packed domains with time revealed that the orientations of some of the crystals also change in a way to maximize the degree of close packing.

The above observation suggests that zeolite crystals initially land on the glass substrate randomly but they do not form strong bonding with the substrates immediately after they land. This suggests that the number of ionic bondings developed between the surface-tethered Bu^- and $TMPA^+$ is not significant. The nature of initial interaction between the zeolite crystals and the substrate may be van der Waals or capillary force. Larger numbers of ionic bondings seem to start developing only when they can stay on the same spot for an extended period time with the help of the closely contacting neighbors. This model seems to be reasonable to explain the ready surface migration and close packing of the zeolite crystals. We proposed a similar mechanism for the close packing of zeolite crystals during the monolayer assembly on glass substrates through AP−fullerene−AP covalent linkages.[7]

In fact, it is interesting that the zeolite crystals ($\mathbf{Z}^+$) undergo close packing despite the fact that their ζ potentials are highly positive (+50) and thus, in principle, coagulation is preventative. This indicates that some sort of short-range attractive force of unknown nature operates between the crystals. Similar short-range attractive forces may operate between the zeolite crystals and the substrates (such as $\mathbf{G}^-$, $\mathbf{G}^+/\mathbf{PSS}^-$, $\mathbf{G}^+/\mathbf{PSS}^-/\mathbf{PDDA}^+/\mathbf{PSS}^-$) in addition to the electrostatic attraction between the opposite charges. However, it can be said that the contribution of the short-range attractive forces to the attractive interaction between zeolite crystals and substrates is not substantial from the observation that the amount of crystals physically adhered to the underlying monolayers of zeolite crystals is small (<10%).

Polyelectrolytes have routinely been employed for the layer-by-layer assembly of two-dimensional platelets, such as clay,[47−50] and the related exfoliated inorganic layered materials,[51] graphite oxide,[52−54] and nanoparticles such as gold,[55] silver,[56−58] silica,[59−61] titania,[62−64] semiconductors,[65,66] and other interesting nanometer-sized materials.[67−71] However, there have been no previous efforts to stratify three-dimensional crystals in micrometer scales. In this respect, the present report demonstrates the expansion of the size limit of the building block to micrometer scales. Considering that the surface area-to-weight ratios of micrometer-sized zeolite crystals are much smaller than those of the ultrathin platelets and nanoparticles, the micrometer-sized zeolite crystals are conceived to be more difficult to assemble on supports through layer-by-layer assembly using very thin molecular glues. Multilayer assembly of micrometer-sized building blocks beyond pentalayers will be feasible, provided that the surfaces of the building blocks are highly flat and the sizes and shapes are highly uniform. We believe it is also possible to assemble multilayers of different types of zeolite and the same type of zeolite crystals with different intercalated compounds that could be exploited for exploration of a variety of new types of chemistry.

In summary, this report demonstrates the facile multilayer assembly of micrometer-sized ZSM-5 crystals on glass substrates by ionic linkages mediated by multilayers of oppositely charged polyelectrolytes. The zeolite crystals in each layer show a strong tendency to closely pack. The binding strength increases with increasing the number of layers of polyelectrolytes as the ionic linker. The presence of full-fledged charge centers tethered to surfaces of zeolite and glass and on the polyelectrolyte linkers is crucial for the layer-by-layer assembly. The assembled multilayers of zeolite crystals are expected to be useful in many important applications. The assembly of zeolite crystals on various other types of substrates such as gold, platinum, ITO (indium tin oxide), and vegetal fibers is in progress and the results will be reported elsewhere.

Acknowledgment. We thank the Ministry of Science and Technology (MOST), Korea for supporting this work through the Creative Research Initiatives (CRI) program.

Supporting Information Available: Figures S1−S5 (PDF). This material is available free of charge via the Internet at http://pubs.acs.org.

JA010517Q

(47) Kleinfeld, E. R.; Ferguson, G. S. *Science* **1994**, *265*, 370.
(48) (a) Kotov, N. A.; Haraszti, T.; Turi, L.; Zavala, G.; Geer, R. E.; Dékány, I.; Fendler, J. H. *J. Am. Chem. Soc.* **1997**, *119*, 6821. (b) Mamedov, A.; Ostrander, J.; Aliev, F.; Kotov, N. A. *Langmuir* **2000**, *16*, 3941.
(49) Lvov, Y.; Ariga, K.; Ichinose, I.; Kunitake, T. *Langmuir* **1996**, *12*, 3038.
(50) van Duffel, B.; Verbiest, T.; Elshocht, S. V. Persoons, A.; Schryver, F. C. D.; Schoonheydt, R. A. *Langmuir* **2001**, *17*, 1243.
(51) Keller, S. W.; Kim, H.-N.; Mallouk, T. E. *J. Am. Chem. Soc.* **1994**, *116*, 8817.
(52) Cassagneau, T.; Fendler, J. H. *Adv. Mater.* **1998**, *10*, 877.
(53) Cassagneau, T.; Fendler, J. H.; Johnson, S. A.; Mallouk, T. E. *Adv. Mater.* **2000**, *12*, 1363.
(54) Kotov, N. A.; Dékány, I.; Fendler, J. H. *Adv. Mater.* **1996**, *8*, 637.
(55) (a) He, J.-A.; Valluzzi, R.; Yang, K.; Dolukhanyan, T.; Sung, C.; Kumar, J.; Tripathy, S. K. *Chem. Mater.* **1999**, *11*, 3268. (b) Gittins, D. I.; Caruso, F. *Adv. Mater.* **2000**, *12*, 1947.
(56) Patil, V.; Sastry, M. *Langmuir* **2000**, *16*, 2207.
(57) Cassagneau, T.; Fendler, J. H. *J. Phys. Chem. B* **1999**, *103*, 1789.
(58) Joly, S.; Kane, R.; Radzilowski, L.; Wang, T.; Wu, A.; Cohen, R. E.; Thomas, E. L.; Rubner, M. F. *Langmuir* **2000**, *16*, 1354.
(59) (a) Caruso, F.; Möhwald, H. *Langmuir* **1999**, *15*, 8276. (b) Caruso, F.; Lichtenfeld, H.; Giersig, M.; Möhwald, H. *J. Am. Chem. Soc.* **1998**, *120*, 8523. (c) Caruso, F.; Caruso, R. A.; Möhwald, H. *Science* **1998**, *282*, 1111.
(60) Lvov, Y.; Ariga, K.; Onda, M.; Ichinose, I.; Kunitake, T. *Langmuir* **1997**, *13*, 6195.
(61) Chen, K. M.; Jiang, X.; Kimerling, L. C.; Hammond, P. T. *Langmuir* **2000**, *16*, 7825.
(62) Liu, Y.; Wang, A.; Claus, R. *J. Phys. Chem. B* **1997**, *101*, 1385.
(63) Correa-Duarte, M. A.; Giersig, M.; Kotov, N. A.; Liz-Marzán, L. M. *Langmuir* **1998**, *14*, 6430.
(64) Caruso, F.; Spasova, M.; Susha, A.; Giersig, M.; Caruso, R. A. *Chem. Mater.* **2001**, *13*, 109.
(65) Cassagneau, T.; Mallouk, T. E.; Fendler, J. H. *J. Am. Chem. Soc.* **1998**, *120*, 7848.
(66) Gao, M.; Richter, B.; Kirstein, S.; Möhwald, H. *J. Phys. Chem. B* **1998**, *102*, 4096.
(67) Rosidian, A.; Liu, Y.; Claus, R. O. *Adv. Mater.* **1998**, *10*, 1087.
(68) Lvov, Y.; Munge, B.; Giraldo, O.; Ichinose, I.; Suib, S. L.; Rusling, J. F. *Langmuir* **2000**, *16*, 8850.
(69) Ichinose, I.; Tagawa, H.; Mizuki, S.; Lvov, Y.; Kunitake, T. *Langmuir* **1998**, *14*, 187.
(70) Ostrander, J. W.; Mamedov, A. A.; Kotov, N. A. *J. Am. Chem. Soc.* **2001**, *123*, 1101.
(71) Fulda, K.-U.; Kampes, A.; Krasemann, L.; Tieke, B. *Thin Solid Films* **1998**, *327−329*, 752.